GEOPHYSICAL RESEARCH LETTERS, VOL. 40, 1–6, doi:10.1002/grl.50411, 2013

Surface ozone variability and the jet position: Implications for projecting future air quality

Elizabeth A. Barnes[1] and Arlene M. Fiore[2]

Received 20 February 2013; revised 20 March 2013; accepted 24 March 2013.

[1] Changes in the variability of surface ozone can affect the incidence of ozone pollution events. Analysis of multi-century simulations from a chemistry climate model shows that present-day summertime variability of surface ozone depends strongly on the jet stream position over eastern North America. This relationship holds on decadal time scales under projected climate change scenarios, in which surface ozone variability follows the robust poleward shift of the jet. The correlation between ozone and co-located temperature over eastern North America is also closely tied to the jet position, implying that local ozone-temperature relationships may change as the circulation changes. Jet position can thus serve as a dynamical predictor of future surface ozone variability over eastern North America and may also modulate ozone variability in other northern midlatitude regions. **Citation:** Barnes, E. A. and A. M. Fiore (2013), Surface ozone variability and the jet position: Implications for projecting future air quality, *Geophys. Res. Lett.*, *40*, doi:10.1002/grl.50411.

1. Introduction

[2] Climate warming is likely to degrade air quality in many polluted regions but models disagree regionally on the magnitude, and sometimes the sign, of the surface ozone response to projected warming [*Fiore et al.*, 2012; *Jacob and Winner*, 2009; *Weaver et al.*, 2009]. The lack of consistency across studies to date, combined with computational constraints limiting many simulations to only a few years, complicates interpretation of model differences. These differences could reflect diversity in emissions, model internal variability (climate noise), or the regional climate response (including feedbacks from chemistry and emissions) to global warming.

[3] Synoptic variability is known to modulate summertime surface ozone levels at northern midlatitudes [*Vukovich*, 1995], but observationally derived relationships between counts of synoptic variability and high-ozone events are relatively weak [*Leibensperger et al.*, 2008; *Turner et al.*, 2013]. Here we show that representing synoptic activity by the latitude of the jet stream leads to robust relationships between the large-scale flow and the standard deviation of surface ozone (a measure of daily variability) over eastern North America in present-day and future climate scenarios. Thus, the response of the jet to climate warming can provide insight into how regional air quality will change in the future.

2. Methods

[4] We exploit 1330 years of simulated daily surface ozone from a suite of simulations from 1860 to 2100 performed for the fifth Coupled Model Intercomparison Project (CMIP5) using the Geophysical Fluid Dynamics Laboratory (GFDL) Climate Model version 3 (CM3) chemistry climate model [*Donner et al.*, 2011]. Specifically, we analyze the Historical (1860–2005; five-member), RCP4.5 (2006–2100; three-member), and RCP8.5 (2006–2100; one-member) simulations, and a sensitivity simulation, denoted as RCP4.5* (three-member), that has evolving well-mixed greenhouse gases following the RCP4.5 scenario but emissions of aerosol and ozone precursors held constant at 2005 levels. RCP4.5* enables us to separate the impact of climate warming (in all scenarios) from the impact of decreasing ozone precursor emissions on ozone variability. In RCP4.5 and RCP8.5, emissions of the dominant ozone precursor, nitrogen oxides (NO_x), decline by 80% from 2005 to 2100 over eastern North America. CM3 uses climatological isoprene and soil NO_x emissions, rather than interactive emissions driven by local meteorological conditions. However, since our focus is on ozone variability driven by the meteorology, the inclusion of these generally positive feedbacks would likely amplify the relationships reported here. Additional information on the model configurations for each scenario are detailed in Table 3 of *John et al.* [2012].

[5] We focus on summer (JJA), the peak ozone pollution season over eastern North America (ENA; 39°N–58°N, 269°E–294°E; see Figure 2). Observations of maximum daily 8 hour average (MDA8) ozone are from the United States Environmental Protection Agency Clean Air Status and Trends Network (CASTNet). We restrict our analysis to the 23 sites in ENA with at least 80% of the daily JJA data for at least 8 of the 10 years between 1990 and 1999. Due to the nonuniform geographical spacing of the sites, we first zonally average the daily data across the region to a 2° latitude grid (to compare with the 2° latitude by 2.5° longitude grid of the model). MDA8 ozone is calculated from hourly surface ozone fields.

[6] Ozone variability is calculated for each JJA decade as the standard deviation of the daily MDA8 ozone anomalies (92 days × 10 years). Anomalies are calculated by subtracting the calendar-day mean and linear trend over the decade.

Additional supporting information may be found in the online version of this article.

[1]Division of Ocean and Climate Physics, Lamont-Doherty Earth Observatory of Columbia University, Palisades, New York, USA.
[2]Department of Earth and Environmental Sciences and Lamont-Doherty Earth Observatory of Columbia University, Palisades, New York, USA.

Corresponding author: E. A. Barnes, Division of Ocean and Climate Physics, Lamont-Doherty Earth Observatory of Columbia University, Palisades, NY, USA. (eabarnes@ldeo.columbia.edu)

0094-8276/13/10.1002/grl.50411

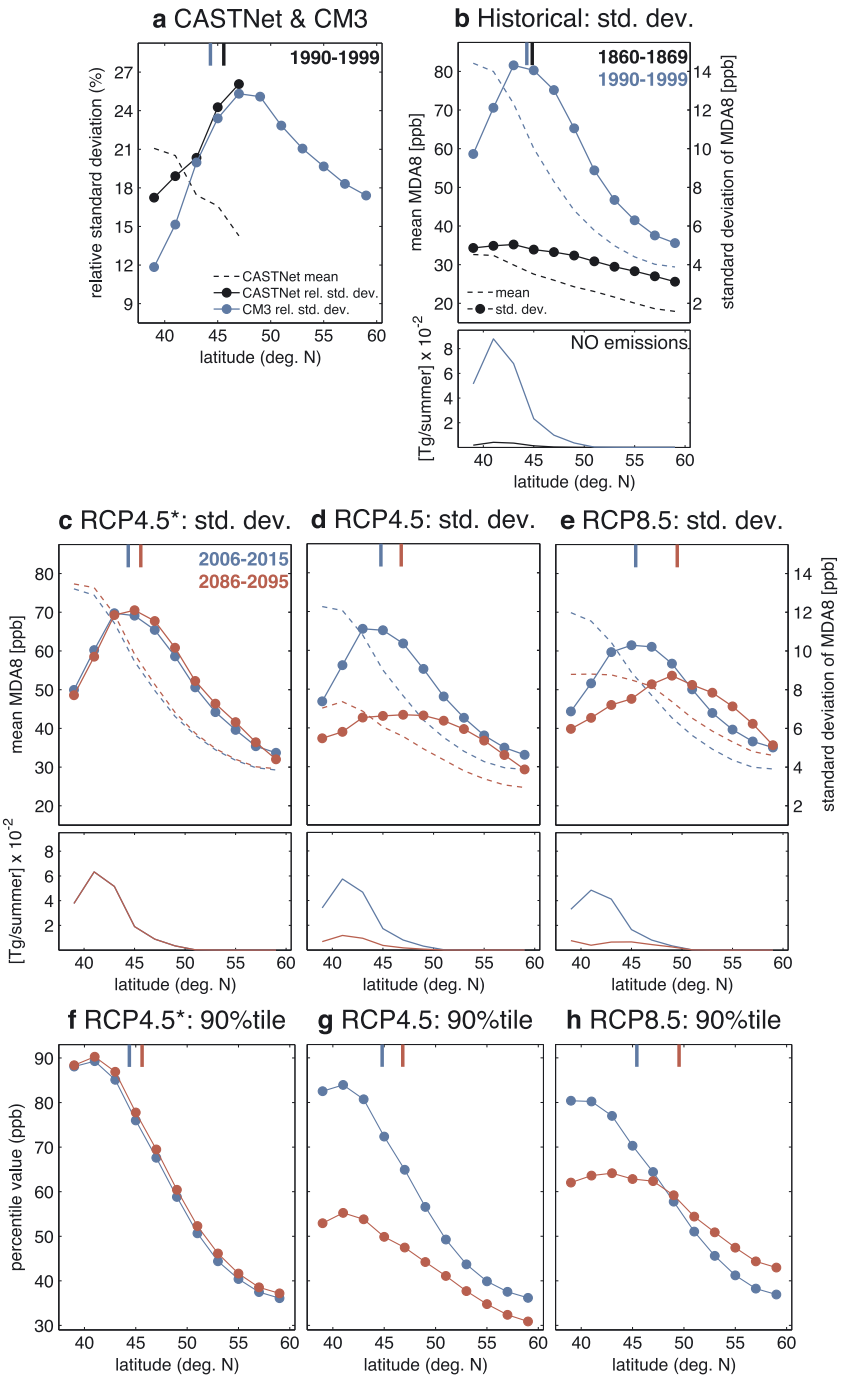

Figure 1. (a) Mean and relative standard deviation of MDA8 ozone over Eastern North America for the CASTNet data set for 1990–1999 and the GFDL CM3 Historical 5-member ensemble average. (b–e) The mean (dashed line) and standard deviation (filled circles) of June-August MDA8 averaged zonally over Eastern North America for (a) CASTNet MDA8 ozone and MERRA-derived jet location and (b–e) GFDL CM3 ensembles with the zonally-integrated surface NO emissions plotted in a separate panel below. (f–h) Meridional distribution of the 90th percentile of MDA8 ozone. The vertical colored bars along the top of each panel denote the mean jet latitude over the period. Colors denote averages over specified time periods.

Unless otherwise stated, we present ensemble-average quantities over each decade where multiple ensemble members are available. The slope of the regression line between MDA8 ozone anomalies and daily maximum 2 m temperature (T_{max}) anomalies is calculated using linear least squares regression as in *Bloomer et al.* [2009], and we report the Pearson correlation coefficient. The jet latitude each summer is defined as the latitude of the maximum 500 hPa JJA zonal winds zonally averaged over ENA. The jet and maximum ozone variability positions are defined from the CM3 model and the Modern Era-Retrospective Analysis for Research and Applications (MERRA) Reanalysis (for our observational analysis) [*Rienecker et al.* 2011] by fitting a quadratic about the peak of the zonally averaged profiles of zonal mean wind and the standard deviation of MDA8 ozone, respectively (see also the supporting information).

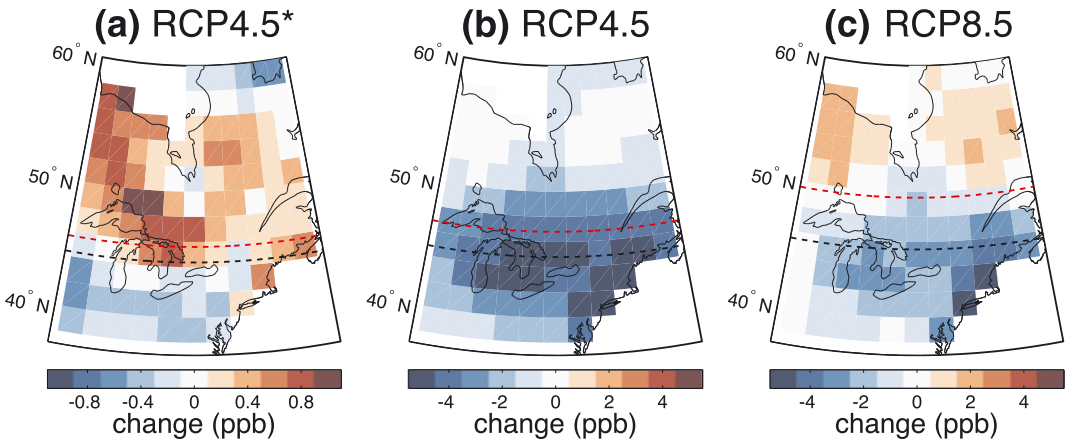

Figure 2. The change in the June–August standard deviation of MDA8 between 2086–2095 and 2006–2015 for the three future scenarios from the model. Dashed lines denote the mean jet latitude for (black) 2006–2015 and (red) 2086–2095 (vertical tick marks in Figure 1).

3. Results

[7] We begin by examining the relationships between the observed mean MDA8 ozone, its standard deviation, and the jet position in Figure 1a. Observed mean MDA8 ozone (dashed line) is maximum over the northeastern United States, near 40°N, where ozone precursor emissions are largest. The largest relative standard deviations of MDA8 ozone (defined as the standard deviation divided by the mean; black dotted line) do not occur in the regions with the largest mean ozone, but instead are offset approximately 5° to the north. This peak in relative ozone variability is located near the location of the 500 hPa jet stream (vertical tick mark along the top of the panel). Note that the 500 hPa level lies approximately 5 km above sea level and thus does not directly measure the surface winds, but rather quantifies the position of the midlatitude jet stream (and storm track).

[8] Model simulated surface ozone (Figure 1b, dashed lines) and its standard deviation (dotted lines) more than doubled between 1860–1869 and 1990–1999 over the northeast United States (40°N–47°N). This doubling reflects the increase in anthropogenic NO_x emissions, the dominant regional ozone precursor (Figure 1b, bottom). While the latitude of the present-day mean ozone maximum is well captured by the Historical model simulations, the model overestimates mean summertime MDA8 ozone over ENA by up to 20 ppb and overestimates preindustrial surface ozone when compared to the limited available observations [e.g., *Horowitz*, 2006]. This overestimate is common among current generation models [*Fiore et al.*, 2009], and the positive bias in mean ozone corresponds to a similar positive bias in ozone variability of up to 20% (see Figure S1). However, the relative standard deviations of MDA8 ozone in the model and the CASTNet observations are similar to within 5% (see Figure 1a), indicating that the model can simulate the processes pertinent to ozone variability.

[9] We hypothesize that a poleward shift of the jet may invoke a similar shift in ozone variability, given their observed and modeled present-day collocation. Figure 2 shows the spatial changes in JJA ozone variability from 2006–2015 to 2086–2095 for the three future scenarios. Ozone variability decreases over the eastern United States and increases over Canada in RCP4.5* and RCP8.5, suggestive of a northward shift. No such increase is found in RCP4.5, although the decrease over the northeast United States aligns with that of RCP8.5. Figures 1c–1e depict the zonal mean changes of Figure 2, and in all three simulations, the latitude of maximum variability between 2006 and 2015 (blue line) aligns with the location of the jet (blue vertical tick marks). By 2086–2095, the jet has shifted northward by 1°–4° (red vertical tick marks; see Figure S2), and the latitude of maximum ozone variability shifts so as to remain aligned with the latitude of the jet.

[10] *Barnes and Polvani* [2013] demonstrate a poleward shift of the North Atlantic jet in JJA across the CMIP5 models, consistent with results shown for CM3. Furthermore, within CM3, the ensemble-mean greenhouse-gas-induced shifts of the jet and maximum ozone variability shown in Figures 1c–1e are all statistically different from zero at 90% confidence using a Monte Carlo approach to estimate the internal variability (see the supporting information and Table S1).

[11] The shift of ozone variability in RCP4.5* (Figure 1c), where ozone precursors are fixed, demonstrates that NO_x emission decreases in RCP4.5 and RCP8.5 are not solely responsible for driving the northward shift of ozone variability. The smaller jet shift in RCP4.5* reflects weaker surface warming than in RCP4.5 where cooling aerosols are removed. Although the NO_x emission decreases in RCP4.5 reduce the variability throughout the region, the location of maximum variability consistently aligns with the jet latitude. For 2086–2095, the mean ozone and standard deviation in RC8.5 are larger than in RCP4.5, likely reflecting the availability of higher baseline free tropospheric ozone due to the doubling of global methane in RCP8.5 (versus a 10% decrease in RCP4.5).

[12] Changes in ozone variability can influence the extremes. Figure 1f shows changes in the 90th percentile toward higher MDA8 ozone values in RCP4.5*, which could reflect a combination of the jet shift and decreased PAN (peroxyacetyl nitrate) production [e.g., *Doherty et al.*, 2013]. For RCP4.5 (Figure 1g), NO_x decreases reduce the extremes at all latitudes. Despite the similar NO_x reductions in RCP8.5, the 90th percentile values increase north of 50°N in RCP8.5 (Figure 1h), likely due to the larger

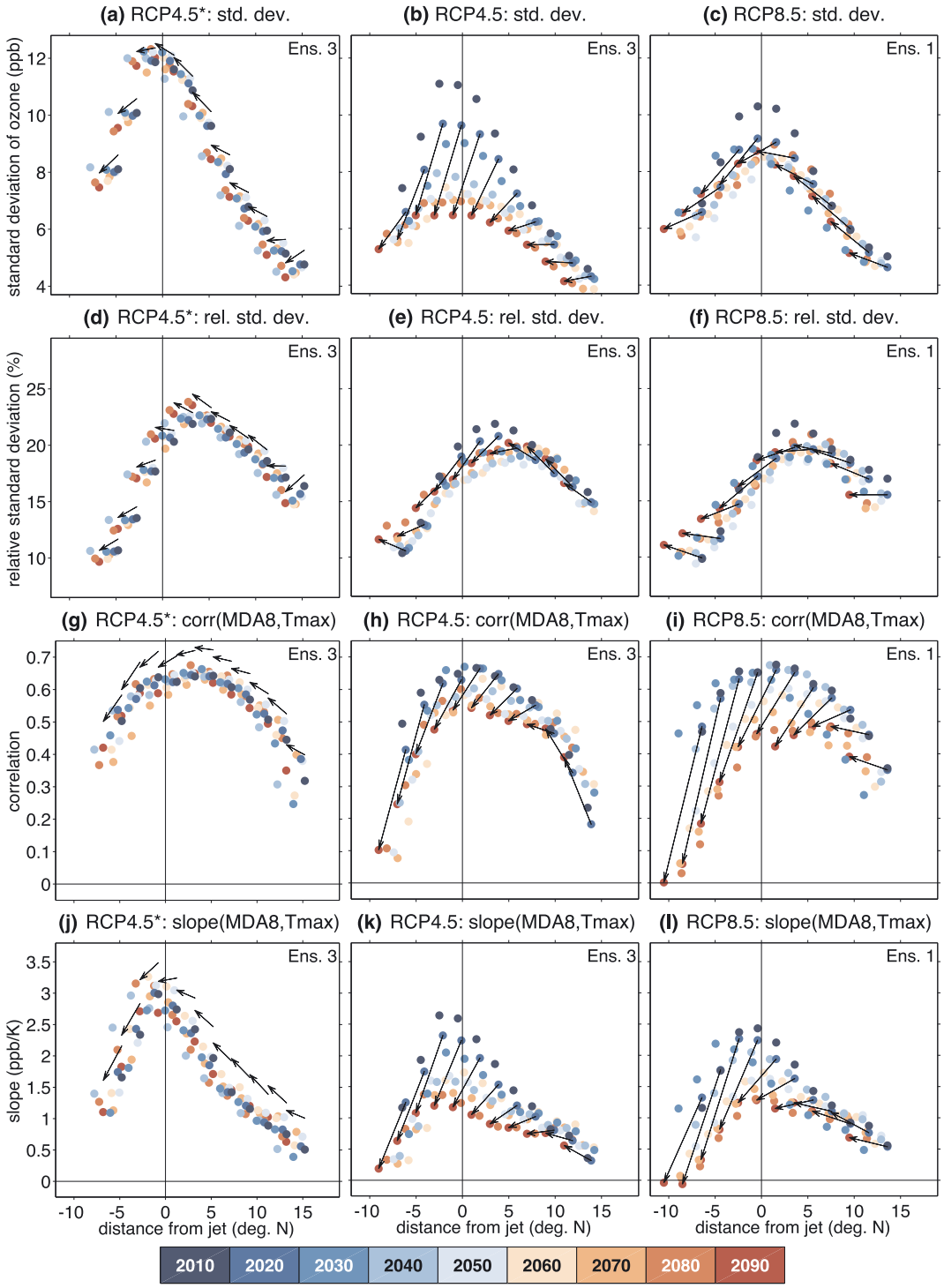

Figure 3. (a–c), The standard deviation of MDA8 zonally averaged over eastern North America plotted against the relative distance from the jet. (d–f) Same as Figures 3a–3c but for the relative standard deviation. (g–i) Similar to Figures 3a–3c except for the correlation between MDA8 and T_{max} anomalies. (j–l) Similar to Figures 3a–3c except for the slope between MDA8 and T_{max} anomalies. Colors denote the decade associated with each value. Arrows connect 2016–2025 (2006–2015 for Figures 3a, 3d, 3g, and 3j) to 2086–2095 for the same geographical location, representing the change between the beginning and end of the 21st century. Panels show results for one ensemble member of each experiment and arrows in Figures 3a, 3d, 3g, and 3j are shifted upward to aid in visualization.

shift of the jet and the smaller decrease in mean ozone compared to RCP4.5.

[13] The relative position of the jet to a given location largely explains the fluctuations of summertime surface ozone there on decadal time scales. We separate the data into 10 year periods, denoted by color, and Figures 3a–3c show ozone variability at each latitude as a function of the distance from the jet. Results for one ensemble of each scenario are

shown since we wish to highlight that the natural variability of the jet position can also influence ozone variability. The peak in ozone variability is found at the latitude of the jet in all decades in Figures 3a–3c (i.e., at zero), demonstrating that fluctuations of the jet position lead to similar fluctuations in ozone variability.

[14] To demonstrate the response of the jet and ozone variability to climate change, arrows in Figure 3 connect the early and late 21st century values for the same geographical location to show the local change in ozone variability. Because NO_x emissions decrease to one third of their initial value over 2006–2015 in RCP4.5 and RCP8.5, we have chosen to highlight the 2016–2025 period. In RCP4.5*, the arrows, and thus the changes in ozone variability, point along the climatological curve, such that when the jet moves closer to a region (northward in the RCP scenarios), ozone variability increases, while in regions further from the jet, ozone variability decreases. Similarly, the jet shifts north by 4° latitude in RCP8.5 and the peak in ozone variability shifts along with it. In RCP4.5, the maximum in ozone variability in every decade is located at the jet latitude, but there are large decreases in the magnitude of the standard deviations, likely due to decreasing mean ozone with emission reductions. The effects of the mean ozone response to emissions can be removed by calculating the relative standard deviation, shown in Figures 3d–3f. All three simulations show that the northward jet shift increases relative ozone variability to the north and decreases ozone variability to the south. That the relative standard deviation peaks north of the jet is purely arithmetic and reflects the influence of lower mean MDA8 ozone (denominator) at higher latitudes.

[15] The relationship between surface ozone variability and the latitude of the jet in a warming climate is summarized in Figure 4. The ensemble-average decadal-mean jet latitude and latitude of maximum ozone variability are highly correlated, where the best fit slope of 1.02 implies that as the jet shifts poleward with climate warming, ozone variability may shift poleward a similar amount.

[16] Relationships between temperature and surface ozone have previously been used to quantify the combined effects of meteorological and temperature-dependent chemical and emission processes on regional air quality [*Bloomer et al.*, 2009]. Given that the jet is strongly tied to synoptic eddy activity (which ozone-temperature correlations implicitly include), it is logical that the jet position is also related to the daily ozone-temperature relationship. The correlations and slopes between MDA8 ozone and T_{max} displayed in Figures 3g–3l are highest near the jet axis and decrease as one moves away from the jet. This is consistent with the notion that the inverse of temperature largely acts as a proxy for synoptic activity, with warmer temperatures implying more stagnant conditions. Additionally, *Bloomer et al.* [2009] demonstrated empirically that the slope between ozone and temperature increases with NO_x, and the influence of NO_x levels on the slope can be seen for RCP4.5 and RCP8.5, while the shift in the circulation explains the variations in the slope for RCP4.5*. With increasing greenhouse gases and a northward jet shift (follow arrows in Figures 3g–3i), larger correlations occur in regions close to the jet, and smaller correlations occur in regions further away where temperature has little linear predictive capability ($R^2 < 25\%$). The correlations decrease substantially in RCP8.5 at most latitudes (Figure 3i), but the standard deviation of ozone does not (see Figure 3c), highlighting that ozone may still be influenced by synoptic activity in the future, but the ability of surface temperature to explain such variations will decrease substantially under this scenario.

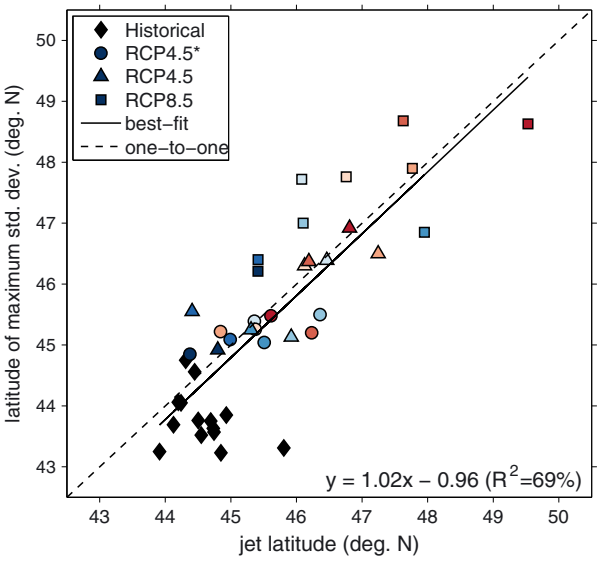

Figure 4. Latitude of the maximum standard deviation of ozone versus jet latitude over ENA for 10 year periods in the Historical and future model simulations. Each point denotes the ensemble mean over the time period when available. Colors denote decades as in Figure 3.

4. Conclusions

[17] The strong dependence of surface ozone variability on jet latitude, a quantity easily computed from climate models, implies that understanding future changes in jet location can be used to derive changes in summertime surface ozone variability and ozone-temperature relationships. Previous studies have suggested that observed regional regressions can be used to predict changes in ozone, given projected changes in temperature or other meteorological variables [*Bloomer et al.*, 2009]. However, our results show that changes in the large-scale tropospheric flow over eastern North America can alter these relationships. Thus, local regressions will likely produce unreliable projections of future ozone if the large-scale circulation shifts with climate warming. Our results further suggest that the ubiquitous discrepancies in jet location [*Barnes and Polvani*, 2013] among climate models may contribute to the wide range of current estimates for climate-driven changes in surface ozone at northern midlatitudes [*Fiore et al.*, 2012; *Weaver et al.*, 2009].

[18] **Acknowledgments.** We acknowledge L. Horowitz, A. Turner, and G. Correa for the model simulations and data support. We also acknowledge the Global Modeling and Assimilation Office (GMAO) and the GES 547 DISC for dissemination of MERRA, the NOAA Climate and Global Change Fellowship (E.A.B), and the EPA-STAR grant 83520601 (A.M.F). The contents of this paper are solely the responsibility of the grantee and do not necessarily represent the official view of the EPA. We thank two anonymous reviewers for their comments.

[19] The Editor thanks two anonymous reviewers for their assistance in evaluating this paper.

References

Barnes, E. A., and L. M. Polvani (2013), Response of the midlatitude jets and of their variability to increased greenhouse gases in the CMIP5 models, *J. Climate*, in press.

Bloomer, B. J., J. W. Stehr, C. A. Piety, R. J. Salawitch, and R. R. Dickerson (2009), Observed relationships of ozone air pollution with temperature and emissions, *Geophys. Res. Lett.*, *36*, L09803, doi:10.1029/2009GL037308.

Doherty, R., O. Wild, D. Shindell, and G. Zeng (2013), Impacts of climate change on surface ozone and intercontinental ozone pollution: A multi-model study, *J. Geophys. Res.*, in press, doi:10.1002/jgrd.50266.

Donner, L. J., et al. (2011), The dynamical core, physical parameterizations, and basic simulation characteristics of the atmospheric component AM3 of the GFDL global coupled model CM3, *J. Climate*, *24*, 3484–3519, doi:10.1175/2011JCLI3955.1.

Fiore, A. M., et al. (2009), Multimodel estimates of intercontinental source-receptor relationships for ozone pollution, *J. Geophys. Res.*, *114*, D04 301, doi:10.1029/2008JD010816.

Fiore, A. M., et al. (2012), Global air quality and climate, *Chem. Soc. Rev.,* in press, *41*(2), 6663–6683, doi:10.1039/c2cs35095e.

Horowitz, L. W. (2006), Past, present, and future concentrations of tropospheric ozone and aerosols: Methodology, ozone evaluation and sensitivity to aerosol wet removal, *J. Geophys. Res.*, *111*, D22 211, doi:10.1029/2005JD006937.

Jacob, D. J., and D. A. Winner (2009), Effect of climate change on air quality, *Atmos. Environ.*, *43*, 51–63.

John, J. G., A. M. Fiore, V. Naik, L. W. Horowitz, and J. P. Dunne (2012), Climate versus emission drivers of methane lifetime from 1860–2100, *Atmos. Chem. Phys.*, *12*, 12021–12036, doi:10.5194/acp-12-12021-2012.

Leibensperger, E. M., L. J. Mickley, and D. J. Jacob (2008), Sensitivity of US air quality to mid-latitude cyclone frequency and implications of 1980–2006 climate change, *Atmos. Chem. Phys.*, *8*, 2075–7086.

Rienecker, M., et al. (2011), MERRA: NASA's Modern-Era Retrospective Analysis for Research and Applications, *J. Climate*, *24*, 3624–3648.

Turner, A. J., A. M. Fiore, L. W. Horrowitz, V. Naik, and M. Bauer (2013), Summertime cyclones over the Great Lakes Storm Track from 1860–2100: Variability, trends and association with ozone pollution, *Atmos. Chem. Phys.*, *13*, 565–578, doi:10.5194/acp-13-565-2013.

Vukovich, F. M. (1995), Regional-scale boundary layer ozone variations in the eastern United States and their association with meteorological variations, *Atmos. Environ.*, *29*, 2259–2273.

Weaver, C. P., et al. (2009), A preliminary synthesis of modeled climate change impacts on U.S. regional ozone concentrations, *Bull. Amer. Meteor. Soc.*, *90*, 1844–1863, doi:10.1175/2009BAMS2568.1.

SUPPLEMENTARY MATERIAL

Surface ozone variability and the jet position: Implications for projecting future air quality

Elizabeth A. Barnes[1] and Arlene M. Fiore[2]

[1]Division of Ocean and Climate Physics, Lamont-Doherty Earth Observatory of Columbia University, Palisades, NY, USA.
[2]Department of Earth and Environmental Sciences and Lamont-Doherty Earth Observatory of Columbia University, Palisades, NY, USA.

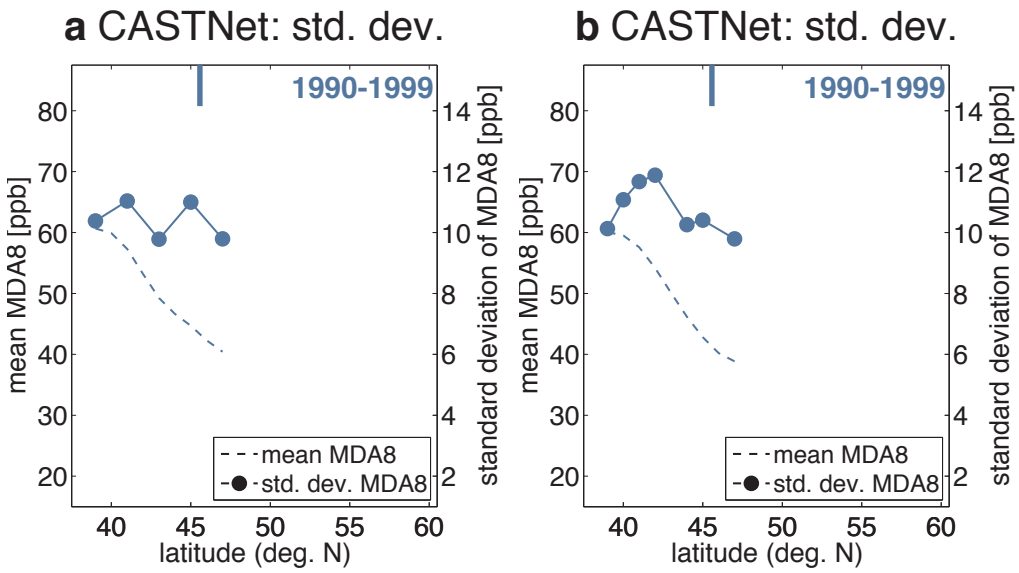

Supplementary Figure 1: The mean (dashed line) and standard deviation (filled circles) of June-August MDA8 averaged zonally over Eastern North America for CASTNet MDA8 ozone and MERRA-derived jet location. (a) Averaging sites over a 2° grid to compare with the GFDL CM3 model and (b) averaging over a 1° grid to show sensitivity to grid size. The number of stations averaged from south to north in (a) 10, 7, 3, 2, 1 and (b) 6, 6, 4, 2, 3, 1, 1.

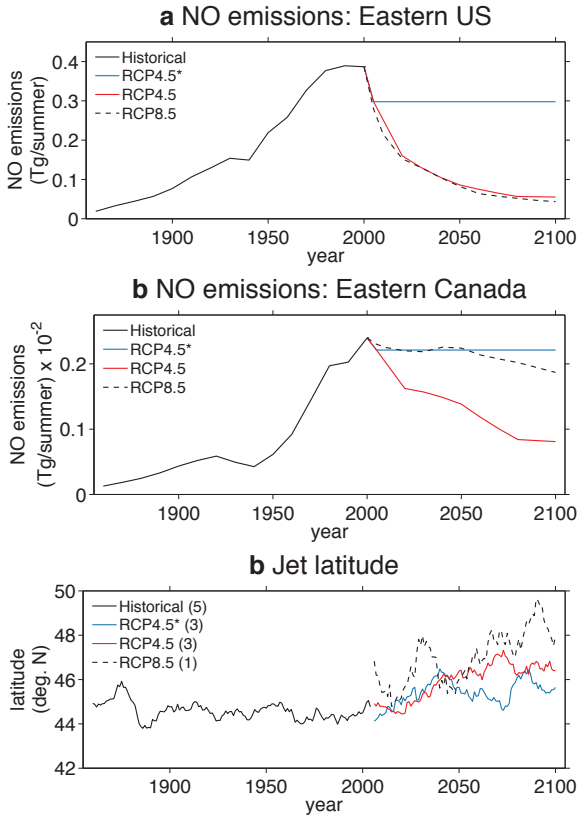

Supplementary Figure 2: Summer-time (JJA) NO emissions for the (a) Eastern US and (b) Eastern Canada regions. Note the different y-axis scalings. (c) Mean jet position over Eastern North America. The jet latitude has been smoothed with a 10-year moving window. Parentheses denote the number of ensembles in each experiment.

Calculation of the jet position

The latitude of the monthly-mean jet position over Eastern North America is defined as the latitude of 500 hPa maximum zonal-mean zonal winds (u) averaged over the sector. Typically, the eddy-driven, midlatitude jet is defined using lower-tropospheric winds in order to distinguish it from the zonal winds associated with the subtropical jet (Barnes and Polvani, 2013; Woollings et al., 2010). The subtropical jet winds increase with height, with easterlies near the surface, whereas the eddy-driven winds are largely barotropic, with westerlies near the surface. Thus, lower-tropospheric winds exhibit a jet peak associated with the midlatitude jet, but not the subtropical jet. Here, we use 500 hPa instead of the lower-troposopheric winds in order to ensure that we are not finding a relationship between the jet location and ozone variability purely because we use near-surface winds and near-surface ozone. The 500 hPa level thus allows us to still distinguish the eddy-driven and subtropical jets, but is also well-removed from the surface.

For each month, the latitude of maximum zonal-mean zonal wind is found, and then the wind profile is interpolated to a 0.01° latitude grid and a quadratic is fit about the maximum. The jet position is defined as the latitude of the maximum interpolated zonal-mean zonal wind. As an example, the figure below shows the sector-averaged zonal wind for August 1998. The black dotted line shows the original MERRA profile, the red curve denotes the fitted quadratic at the peak, and the star denotes the position of the jet defined according to the methodology outlined above. Note that even though the resolution of the data is 2° latitude, the latitude of the jet can be defined up to much higher precision since monthly zonal wind is a continuous and smooth variable.

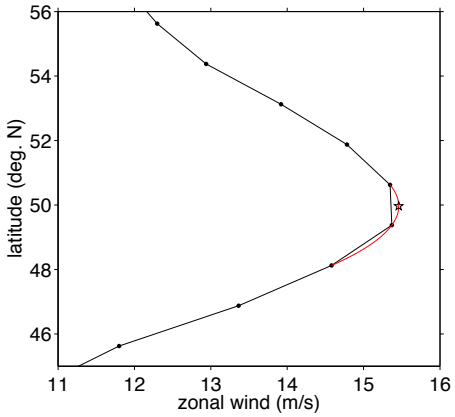

Supplementary Figure 3: Zonally averaged 500 hPa zonal winds over Eastern North America for August 1998 from MERRA. The red curve denotes the fitted quadratic at the peak and the star depicts the position of the jet.

Calculation of the position of maximum ozone variability

We define the latitude of the seasonal-mean ozone variability by finding the latitude of maximum variability each season of each year. Similar to the jet, the latitude of the maximum ozone variability is found, and then the profile is interpolated to a 0.01° latitude grid and a quadratic is fit about the maximum. The position of maximum ozone variability is then defined as the latitude of the interpolated field maximum.

Estimating the significance of shifts

The natural variability of the jet position is calculated using a Monte Carlo approach by randomly sampling 10,000 10-year groups from the 5 Historical ensemble members. We follow a similar process for the peak in ozone variability, except we use the 3 RCP4.5* ensemble members to ensure the shifts are not due to emission changes.

	RCP4.5*		RCP4.5		RCP8.5	
	Δjet	$\Delta\sigma_{O_3}$	Δjet	$\Delta\sigma_{O_3}$	Δjet	$\Delta\sigma_{O_3}$
Ens. 1	0.6^o	0.3^o	**3.1**^{o}	**2.9**^{o}	**4.1**^{o}	**3.3**^{o}
Ens. 3	**2.0**^{o}	**1.0**^{o}	**2.5**^{o}	**2.9**^{o}	-	-
Ens. 5	1.1^o	**0.8**^{o}	0.4^o	**3.2**^{o}	-	-
Ens. Avg.	**1.2**^{o}	**0.7**^{o}	**2.0**^{o}	**3.0**^{o}	**4.1**	**3.3**

Supplementary Table 1: Simulated meridional shifts (in degrees north) of the jet and the maximum MDA8 ozone variability (σ_{O_3}) between 2006-2015 and 2086-2095 in each ensemble for the three future scenarios. Bold values denote shifts statistically different from zero at 90% confidence using a Monte Carlo approach.

References

Barnes, E. A. and L. M. Polvani, 2013: Response of the midlatitude jets and of their variability to increased greenhouse gases in the CMIP5 models. *J. Climate*, **in press**.

Woollings, T., A. Hannachi, and B. Hoskins, 2010: Variability of the North Atlantic eddy-driven jet stream. *Quart. J. Roy. Meteor. Soc.*, **136**, 856–868, doi:10.1002/qj.625.